Wind Tunnel Wall Interference Corrections for Aircraft Models in the Transonic Regime

Magdi H. Rizk* and Earll M. Murman†
Flow Industries, Inc., Kent, Washington

A procedure for the evaluation of wall interference corrections for three-dimensional models is presented. In addition to Mach number and angle-of-attack corrections, the procedure provides an estimate of the accuracy of the corrections. Lift, pitching moment, and pressure measurements near the tunnel walls are required by the correction method. The method is demonstrated by application to an isolated wing model and to a wing-body-tail configuration.

Nomenclature

c = characteristic chord length
E_L = defined in Eq. (1a)
E_M = defined in Eq. (3)
E_m = defined in Eq. (1b)
$E_{\alpha,t}$ = defined in Eq. (2c)
$E_{\alpha,w}$ = defined in Eq. (2b)
e_M = defined in Eq. (6)
L = lift/P_0c^2
ℓ = lift spanwise distribution/P_0c^2
M = Mach number
m = Pitching moment about the axis $x=x_m/P_0c^3$
P_0 = total pressure
$\boldsymbol{P}$ = $(M_{F\infty}, \alpha_{F,w}, \alpha_{F,t})$
p = $(\alpha_{T,w}, \alpha_{T,t})$
R = residual
X = x coordinate relative to the wing leading tip
x, y, z = Cartesian coordinate system
x_m = x coordinate of axis about which the model pitching moment is measured
Y = y coordinate normalized by the wing semispan
α = angle of attack
γ = ratio of specific heats
ΔM = Mach number correction
$\Delta\alpha$ = angle-of-attack correction
ϵ = small positive number determining convergence
ρ = density
Φ = perturbation velocity potential for the free-air flow
ϕ = perturbation velocity potential for the tunnel flow

Subscripts and Superscripts

d = model
e = measured quantity or experimental condition
F = calculated quantity for the equivalent model in an inviscid free-air flow
f = corrected condition
M = Mach number
n = number of iterations
R = residual
s = shock wave
T = calculated quantity for the equivalent model in an inviscid tunnel flow
t = tail
w = wing
∞ = undisturbed condition
$*$ = optimum value

Received Jan. 21, 1983; revision received June 13, 1983.

*Senior Research Scientist, Research and Technology Division. Member AIAA.

†Professor, Massachusetts Institute of Technology, Cambridge, Mass. Associate Fellow AIAA.

Introduction

WALL interference effects are a limiting factor on the accuracy of data obtained from transonic wind tunnel tests. It is well-known that ventilated test section walls (either porous or slotted) are necessary to reduce blockage effects at Mach numbers close to unity. However, wall effects on flow around the model introduce uncertainty errors into the data. Classical linear theory[1] provides an insight into the nature of these errors. For example, it is known that the pressures (and hence the forces) on a model tested at a tunnel Mach number $M_{e\infty}$ and geometric angle of attack α_e are closer to those that the same model would experience at a freestream Mach number $M_{f\infty}=M_{e\infty}+\Delta M$ and angle of attack $\alpha_f=\alpha_e+\Delta\alpha$. The blockage ($\Delta M$) and lift ($\Delta\alpha$) corrections represent only the dominant effects. Higher-order corrections are needed for models of realistic size relative to the tunnel dimensions.

Although classical wall interference theory provides an insight into the features of wall interference, it does not produce sufficiently accurate formulas for practical use. Its limitations include 1) the modeling of the ventilated wall by the general homogeneous wall boundary condition; 2) the assumption that the model is small compared to the tunnel size; 3) the assumption of an infinitely long test section; and 4) the neglect of transonic flow effects. Most wind-tunnel installations, therefore, use experimentally determined correction formulas that retain some functional relationships from classical theory. The uncertainty of the corrections is often so great that no corrections at all are applied. It is also not clear from the theory whether corrections are always possible. One can imagine conditions where the transonic flow in the tunnel does not correspond to any free-air flow. Classical theory provides no suitable estimation of the accuracy of the correction.

Two recently proposed wall correction procedures are now in the research stage. One of these procedures uses adaptive wall tunnels[2,3] to eliminate the wall interference in situ. This approach combines tunnel measurements and computational analysis to determine a wall setting that corresponds to a free-air streamline. In principle, experiments in an adaptive wall tunnel may be rendered completely free of wall interference. The method has been demonstrated using blowing and suction through segmented porous walls,[4-7] through segmented slotted walls,[8] and through deforming or compliant solid walls.[9-11] Results to date are quite encouraging. Three-dimensional geometries appear less demanding in terms of the

amount of wall control required to eliminate interference.[5] Nevertheless, the practical limitations of adaptive wall technology are not yet quantified.

The second approach to wall interference was formulated by Kemp[12,13] and involves making post-test corrections together with a quantitative assessment on the error of the corrections. If the error is unacceptably large, a limited amount of adaptive wall control can be employed followed by post-test correction and assessment. Kemp's method uses measured pressures near the wall in lieu of the classical homogeneous wall boundary conditions. Nonlinear transonic computer codes are then employed to determine the corrections ΔM and $\Delta\alpha$ and higher-order effects. Thus many of the shortcomings of classical theory are overcome. The finite-length test section may be incorporated either by approximation or by additional measurement. Murman[14] made improvements in Kemp's formulation and conducted a series of two-dimensional airfoil simulations to show that wall interference corrections are possible for strongly supercritical flows. Recently procedures[15-17] have been developed for the evaluation of wind tunnel wall interference corrections for three-dimensional geometries. These procedures are extensions of the two-dimensional method of Mokry and Ohman[18] to three-dimensional flows. They eliminate the first three limitations of classical theory mentioned above; however, they cannot be applied to strongly supercritical flows, since the flow is assumed to be governed by the linearized equations.

It is premature at present to compare the relative merits of the adaptive wall and correction/assessment approaches, since it is apparent that a spectrum of possibilities exists ranging from complete adaptive wall control to complete post-test correction/assessment analysis. The optimum combination will probably be facility dependent.

This paper presents the results of a study undertaken to extend the Kemp correction/assessment approach to practical three-dimensional geometries and includes a detailed formulation of the procedure, a summary of its basic assumptions and elements, and the computed results. The results, however, are illustrative in nature, as the methodology has not yet been applied to actual tunnel data. One guideline of the research was to develop a procedure that allows a tradeoff between complexity (cost) and accuracy so that a practical choice can be made.

The goal of the procedure is to determine Mach number and angle-of-attack corrections together with a numerical estimate of the error E_M. Observations and physical reasoning indicate that transonic wall interference effects are less severe for three-dimensional geometries than for two-dimensional geometries. Therefore, simplifying assumptions can be made to develop a cost-effective procedure that minimizes the number of measurements needed to assess wall interference and uses sensors installed in the facility rather than in the model.

The experimental data required by the correction procedure include the usual parameters ($M_{e\infty}$ and α_e) and model forces, together with the measurement of one variable at a control surface near the tunnel wall. Although the method is formulated assuming that this is a static pressure, another variable such as vertical velocity[19] could be used equally well. An inviscid transonic code simulating the flow about a simplified representation of the experimental model is used to evaluate the Mach number and angle-of-attack corrections.

An earlier, but less complete version of this work has been presented in Ref. 20. In the present work, the efficiency and accuracy of the correction procedure are improved. Moreover, the present work allows correction of both the wing and tail angle of attacks, while the work described in Ref. 20 allows only one angle-of-attack correction.

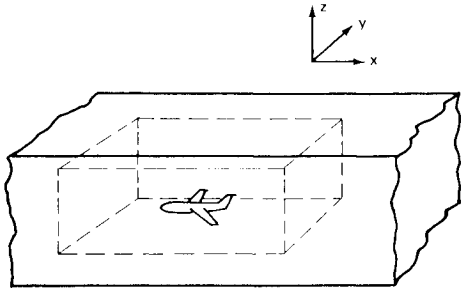

Fig. 1 Geometrical configuration.

Correction Procedure

The correction procedure for a general-aircraft-like test model requires that pressure measurements be made on the boundaries of rectangular parallelepiped with sides close to the tunnel walls but outside the boundary-layer region (see Fig. 1). If the end planes are taken far upstream and far downstream from the model, it may be possible to replace the pressure measurements on these end planes by simple theoretical estimates. The freestream Mach number, the model angle of attack, the lift force, and the pitching moment are also required by the correction procedure. An inviscid transonic code simulating the flow about a simplified model uses the experimental data to evaluate the lowest-order wall interference corrections, ΔM and $\Delta\alpha$. The correction procedure is divided into the two steps described below.

In the first step, an equivalent model is determined such that it suitably represents the tested geometrical model together with corrections for viscous effects. It is not required that the equivalent model produce the detailed flow features of the tested model. However, the dominant or global flow features produced by the model tested in the wind tunnel must correspond with features produced by the equivalent model in an inviscid wind tunnel. The correction procedure requires

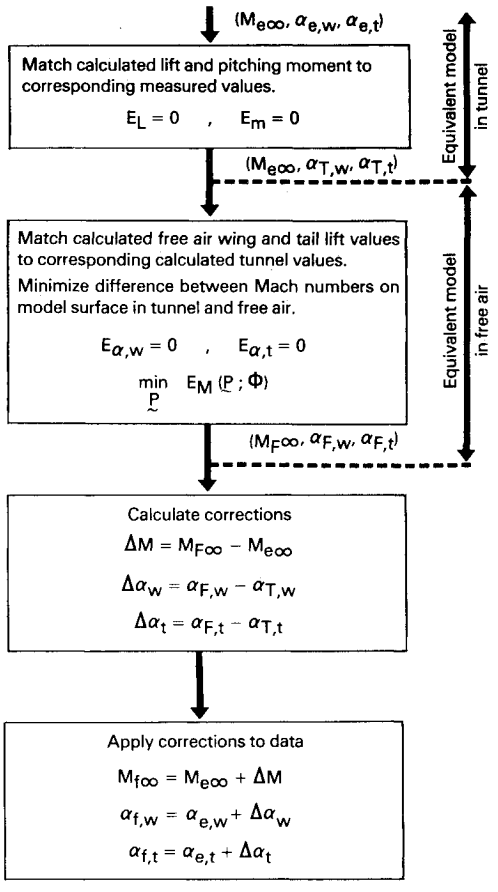

Fig. 2 Correction procedure.

that the flow be calculated numerically about the equivalent model. Therefore the equivalent model should be simple enough to allow numerical calculation of the flow about it at a reasonable cost. The wing and tail angles of attack, $\alpha_{T,w}$ and $\alpha_{T,t}$, are determined such that the calculated lift and pitching moment of the equivalent model are respectively equal to the measured lift and pitching moment of the tested model. The problem solved in this step may be stated as follows: Find $p\,[=(\alpha_{T,w}, \alpha_{T,t})]$ subject to the constraints:

$$E_L \equiv E_{L,d}(p;\phi) \equiv \frac{L_{T,d}(p;\phi) - L_{e,d}}{L_{e,d}} = 0 \tag{1a}$$

$$E_m \equiv E_{m,d}(p;\phi) \equiv \frac{m_{T,d}(p;\phi) - m_{e,d}}{m_{e,d}} = 0 \tag{1b}$$

with ϕ satisfying the equation

$$D(\phi;M_{e\infty}) = 0 \tag{1c}$$

subject to the boundary conditions

$$b_1(\phi) = 0 \tag{1d}$$

$$b_2(\phi;\alpha_{T,w},\alpha_{T,t}) = 0 \tag{1e}$$

Equation (1c) is the full potential equation

$$\nabla \cdot [\rho \nabla (x+\phi)] = 0$$

or an approximation to this equation. In the present work, the transonic small disturbance approximation is used. Therefore

$$D(\phi;M_\infty) = [\rho^{(2)}(1+\phi_x)]_x + (\rho^{(1)}\phi_y)_y + (\rho^{(0)}\phi_z)_z$$

where

$$\rho^{(0)} = 1$$

$$\rho^{(1)} = 1 - M_\infty^2 \phi_x$$

$$\rho^{(2)} = 1 - M_\infty^2 \phi_x - \tfrac{1}{2} M_\infty^2 (\phi_x^2 + \phi_y^2) + \tfrac{1}{2}(2-\gamma) M_\infty^4 \phi_x^2$$

Boundary condition (1d) is the boundary condition at the rectangular parallelepiped surfaces. It consists of Dirichlet boundary conditions specified at the side planes. These conditions are estimated from pressure measurements there. At the two end planes, appropriate boundary conditions are defined. These may either be obtained from experimental measurements (if available) or from theoretical considerations. Boundary condition (1e) specifies zero flow through the model surface.

It should be noted that the angle-of-attack modifications are due both to the viscous effects present in the experiment

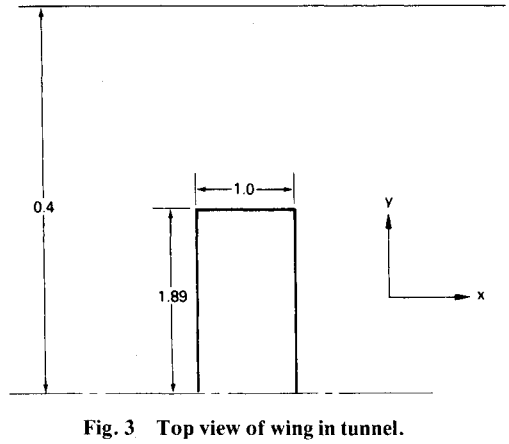

Fig. 3 Top view of wing in tunnel.

but not in the numerical simulation of the flow and to the geometrical differences between the equivalent model and the test model. Additional factors may be included in the simplified equivalent model to account for other viscous effects if needed.

In the second step of the correction procedure, the values of $\alpha_{F,w}$, $\alpha_{F,t}$, and $M_{F\infty}$ are determined such that the values of the equivalent model wing lift in free air and in the tunnel are matched; the values of the equivalent model tail lift in free air and in the tunnel are matched; and the Mach number difference on the equivalent model surface in free air and in the tunnel is minimized. The problem solved in this step may be stated as follows: Find the optimum value of $P\,[=(M_{F\infty}, \alpha_{F,w}, \alpha_{F,t})]$, P^*, such that

$$E_M(P^*;\Phi) = \min_P E_M(P;\Phi) \tag{2a}$$

subject to the constraints

$$E_{\alpha,w}(P;\Phi) \equiv \frac{L_{F,w}(P;\Phi) - L_{T,w}(p;\phi)}{L_{T,w}(p;\phi)} = 0 \tag{2b}$$

$$E_{\alpha,t}(P;\Phi) \equiv \frac{L_{F,t}(P;\Phi) - L_{T,t}(p;\phi)}{L_{T,t}(p;\phi)} = 0 \tag{2c}$$

with Φ satisfying the equation

$$D(\Phi;M_{F\infty}) = 0 \tag{2d}$$

subject to the boundary conditions

$$B_1(\Phi) = 0 \tag{2e}$$

$$b_2(\Phi;\alpha_{F,w}, \alpha_{F,t}) = 0 \tag{2f}$$

Boundary condition (2e) specifies the free-air far field conditions. Here,

$$E_M \equiv \frac{\int (M_F - M_T)^2 \mathrm{d}s}{\int M_T^2 \mathrm{d}s} \tag{3}$$

This is a measure of the Mach number difference on the equivalent model surface in the tunnel and in free air. The integrals are taken over the equivalent model surface. The choice of normalizing the lift by the total pressure allows the calculated values of L in Eqs. (2b) and (2c) to be dependent on the Mach number distribution on the model surface while being independent of the undisturbed Mach number value M_∞.

The Mach number and angle-of-attack corrections are calculated from the relations

$$\Delta M = M_{F\infty} - M_{T\infty} \quad \Delta\alpha_w = \alpha_{F,w} - \alpha_{T,w} \quad \Delta\alpha_t = \alpha_{F,t} - \alpha_{T,t}$$

and the corrected Mach number and angles of attack are then found from the relations

$$M_{f\infty} = M_{e\infty} + \Delta M \quad \alpha_{f,w} = \alpha_{e,w} + \Delta\alpha_w \quad \alpha_{f,t} = \alpha_{e,t} + \Delta\alpha_t$$

An estimate of the accuracy of the wall interference corrections is given by the value of E_M. If E_M exceeds an acceptable value, the data must be considered as uncorrectable. If an adaptive tunnel is available, it may be used to reduce the wall interference in this case. A summary of the correction procedure is given in Fig. 2.

In certain situations it may not be required or desirable to have different wing and tail angle-of-attack corrections. In such cases an alternative approach which determines the values of $\alpha_{F,d}$ and $M_{F\infty}$ may be used in the second step of the correction procedure. These parameters are determined such

that the values of the equivalent model lift in free air and in the tunnel are matched, and the difference in Mach numbers on the equivalent model surface is minimized. In this formulation, Eq. (2b) is deleted, while subscripts t in Eq. (2c) are replaced by subscripts d. The value of $m_{f,d}-m_{e,d}$ in addition to E_M becomes a measure of the accuracy of the wall interference corrections.

Numerical Approach

Step 1: Wind Tunnel Simulation

In this step, the angles of attack $\alpha_{T,w}$ and $\alpha_{T,t}$ are determined. To determine these angles of attack it is necessary to solve problem (1). Reference 21 describes a procedure for solving the transonic small disturbance equation iteratively by successive line overrelaxation. This procedure is used to solve Eq. (1c) with the following modification. In a standard solution of Eq. (1c), the potential function ϕ is updated at the end of each iterative sweep, with the iterative solution ϕ^{n+1} resulting at the end of the $n+1$ iterative sweep. Throughout this process, the values of $\alpha_{T,w}$ and $\alpha_{T,t}$ are held fixed. In the current procedure, the values of $\alpha_{T,w}$ and $\alpha_{T,t}$ are updated before each relaxation sweep by adding the incremental values $\delta\alpha_{T,w}^{n+1}$ and $\delta\alpha_{T,t}^{n+1}$ to the angle-of-attack values at the nth iteration, $\alpha_{T,w}^{n}$ and $\alpha_{T,t}^{n}$. The scheme used for updating the values of the wing and tail angles of attack before the $n+1$ relaxation sweep is given by

$$\alpha_{T,i}^{n+1}=\alpha_{T,i}^{n}+\delta\alpha_{T,i}^{n+1} \qquad i=w,t \tag{4}$$

where

$$\delta\alpha_{T,i}^{n+1}=-\frac{E_{L,i}^{n}}{|E_{L,i}^{n}|}\left[\min\left(C_{\alpha}\,|E_{L,i}^{n}|,A_{\alpha}\right)\right] \qquad i=w,t$$

$$E_{L,i}^{n}=E_{L,i}(\boldsymbol{p}^{n};\phi^{n}) \qquad i=w,t$$

This is the Chord method[22] with an upper limit on the magnitude of $\delta\alpha_{T,i}^{n+1}$ specified by the positive constant A_{α}. C_{α} is a positive constant. Estimates for $L_{e,w}$ and $L_{e,t}$, which are required for the evaluation of $E_{L,w}$ and $E_{L,t}$ are given in the Appendix. In evaluating $E_{L,i}^{n}$, the nth iterative solution, ϕ^{n}, is used. After the values of $\alpha_{T,w}$ and $\alpha_{T,t}$ are updated, a relaxation sweep is performed in order to calculate the new iterative solution, ϕ^{n+1}. The iterative process continues until the convergence criterion

$$\max(|R^{n}|-\epsilon_{R},\ |E_{L,w}^{n}|-\epsilon_{\alpha},\ |E_{L,t}^{n}|-\epsilon_{\alpha})<0$$

is satisfied, where R^{n} is the maximum residual for the set of finite-difference equations at the nth iteration, and ϵ_{R} and ϵ_{α} are small positive constants.

Step 2: Free-Air Simulation

In this step, the angles of attack $\alpha_{F,w}$ and $\alpha_{F,t}$ and the Mach number $M_{F\infty}$ are determined. In order to determine these parameters it is necessary to solve the boundary value problem, Eqs. (2d-2f), subject to constraints (2b) and (2c) and to condition (2a). A procedure similar to the above-described procedure is used here. For free-air simulation, however, each iterative step requires that the values of $\alpha_{F,w}$, $\alpha_{F,t}$, and $M_{F\infty}$ be updated. This is then followed by a relaxation sweep which updates the value of Φ. In the $n+1$ iterative step, the values of $\alpha_{F,w}$ and $\alpha_{F,t}$ are updated as follows:

$$\alpha_{F,i}^{n+1}=\alpha_{F,i}^{n}+\delta\alpha_{F,i}^{n+1} \qquad i=w,t \tag{5}$$

where

$$\delta\alpha_{F,i}^{n+1}=-\frac{E_{\alpha,i}^{n}}{|E_{\alpha,i}^{n}|}\left[\min\left(C_{\alpha}\,|E_{\alpha,i}^{n}|,A_{\alpha}\right)\right] \qquad i=w,t$$

$$E_{\alpha,i}^{n}=E_{\alpha,i}(\boldsymbol{P}^{n};\Phi^{n}) \qquad i=w,t$$

The scheme used for updating the freestream Mach number before the $n+1$ relaxation sweep is described in Ref. 23. This scheme requires the introduction of a new function e_M given by

$$e_M(\boldsymbol{P}^{n};\Phi^{n})=\frac{\int(M_F-M_T)\,ds}{\int M_T\,ds} \tag{6}$$

The scheme is given by

$$M_{F\infty}^{n+1}=M_{F\infty}^{n}+\delta M_{F\infty}^{n+1} \tag{7}$$

$$\delta M_{F\infty}^{n+1}=\tfrac{1}{2}\delta M_{F\infty}^{n}\left[c_1(s^{n}+1)+c_2(s^{n}-1)\right] \tag{8}$$

$$s^{n}=-\frac{F^{n}\delta M_{F\infty}^{n}}{|F^{n}\delta M_{F\infty}^{n}|}$$

$$F^{n}=(E_M^{n}-E_M^{n-1})(e_M^{n}-e_M^{n-1})$$

$$E_M^{n}=E_M(\boldsymbol{P}^{n};\Phi^{n}), \qquad e_M^{n}=e_M(\boldsymbol{P}^{n};\Phi^{n})$$

and c_1 and c_2 are constants with $c_1>1$ and $c_2<1$. Equation (8) determines the sign and magnitude of the incremental value $\delta M_{F\infty}^{n+1}$. The sign of the incremental value is determined in a manner similar to that used in Ref. 20. However, the magnitude is determined in the manner suggested by Kemp during a recent visit to NASA Langley Research Center. When the sign of $\delta M_{F\infty}^{n+1}$ is in agreement (disagreement) with the sign of $\delta M_{F\infty}^{n}$, the magnitude of $\delta M_{F\infty}^{n+1}$ is increased (decreased) by the factor c_1 (c_2) relative to the magnitude of $\delta M_{F\infty}^{n}$. The scheme used in determining the magnitude of $\delta M_{F\infty}^{n+1}$ in Ref. 20 proved to be unreliable.

After the values of $\alpha_{F,w}$, $\alpha_{F,t}$, and $M_{F\infty}$ are updated, a relaxation sweep is performed to calculate the new iterative solution Φ^{n+1}. The iterative process continues until the convergence criterion

$$\max(|R^{n}|-\epsilon_{R},\ |E_{\alpha,w}^{n}|-\epsilon_{\alpha},\ |E_{\alpha,t}^{n}|-\epsilon_{\alpha},\ |\delta M_{F\infty}^{n}|-\epsilon_{M})<0$$

is satisfied.

Results and Discussion

The correction procedure described above is applied to a rectangular wing, with a NACA 0012 airfoil section, located in the middle of a solid-wall wind tunnel of height 3.26 (see Fig. 3). The flow in the wind tunnel is assumed to be inviscid with an undisturbed Mach number value of 0.8, while the value of the lift experienced by the wing is assumed to be $L=0.343$. In the case of a model with only one lifting surface, the correction procedure does not require the pitching moment. The first step of the correction procedure determines the value of the wind tunnel angle of attack ($\alpha_T=2.768$ deg), while the second step determines the values of the corrected

Table 1 Comparison of results based on linear theory to those based on transonic theory

	$\Delta\alpha$	ΔM	$\lvert E_M\rvert$	$\lvert E_{\alpha,w}\rvert$
Uncorrected conditions	0	0	0.272×10^{-2}	0.222
Linear theory	0.550 deg	0.004	0.644×10^{-3}	0.395×10^{-1}
Transonic theory	0.593 deg	0.009	0.916×10^{-4}	0.116×10^{-5}

Mach number ($M_{F\infty}=0.809$) and the corrected angle of attack ($\alpha_F=3.361$ deg). In calculating this example, the pressure boundary condition (1d) has been replaced by a solid-wall boundary condition.

A comparison between the results of the present procedure and linear theory is given in Table 1. In calculating $\Delta\alpha$ and ΔM by linear theory the present approach has been used after setting

$$D(\phi;p)=(1-M_\infty^2)\phi_{xx}+\phi_{yy}+\phi_{zz}$$

The table indicates inaccuracies in the linear results. Although linear corrections may be used with good accuracy for subcritical flows, a fast deterioration in accuracy occurs for supercritical flows as the size of the supersonic region increases.[24] The values of $|\partial E_M|$ and $|E_{\alpha,w}|$ shown in the table are calculated using solutions of the transonic equation at the uncorrected condition and at conditions corrected by linear theory and transonic theory.

A comparison between the spanwise lift distribution for the wind tunnel flow ($M_\infty=0.8$, $\alpha=2.768$ deg), the free-air flow at the uncorrected conditions ($M_\infty=0.80$, $\alpha=2.768$ deg), the free-air flow at the corrected conditions ($M_\infty=0.809$, $\alpha=3.361$ deg), and the free-air flow at the conditions corrected by linear theory ($M_\infty=0.804$, $\alpha=3.318$ deg), is given in Fig. 4. Figure 5 shows the Mach number distributions on the wing top surface at the midsemispan station. A comparison between the shock wave locations for the different flow conditions is shown in Fig. 6.

Scheme (5) for determining α subject to constraint (2b) effectively accelerates the rate of convergence for solving the flow equation.[24] Scheme (7) for determining M_∞ subject to condition (2a), however, does not have a strong effect on the convergence properties for solving the flow equation.[23] To determine the effect of using both schemes simultaneously, as described above, on the rate of convergence of the flowfield solution, a standard calculation with $M_{F\infty}=0.809$ and $\alpha_F=3.361$ deg was performed. In this calculation, $\boldsymbol{P}$ was not updated during the iterative process. A solution obtained on a coarse computational mesh was used as an initial guess for solving the problem on the final mesh. The number of iterations required for convergence ($\epsilon_R=0.0005$) of the standard iterative process is 124 iterations for the coarse mesh and 223 iterations for the fine mesh. The corresponding number of iterations required for convergence ($\epsilon_R=0.0005$, $\epsilon_M=10^{-6}$, $\epsilon_\alpha=10^{-5}$) of the present iterative process is 116 iterations for the coarse mesh and 205 iterations for the fine mesh, indicating comparable, but slightly better convergence properties for the present iterative process.

In the above calculations, the initial guess for the values of $M_{F\infty}$ and α_F were taken to be 0.83 and 3.0 deg, respectively. The intial incremental value $\delta M_{F\infty}^l$ and the constants c_1, c_2, and C_α were set equal to 0.002, 1.2, 0.6, and 3.0, respectively. No attempt has been made to optimize the values of these parameters in the present calculations.

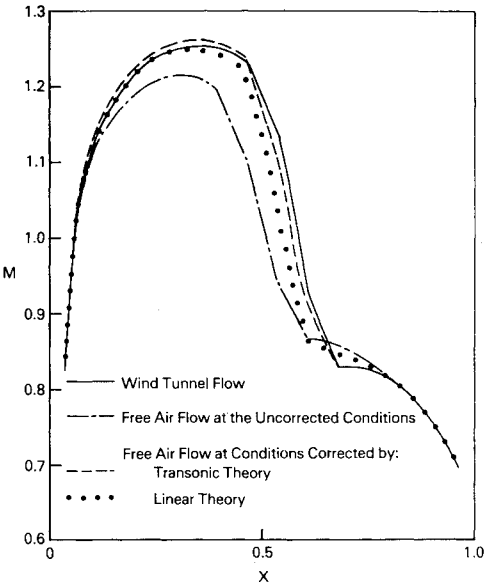

Fig. 5 Mach number distribution on wing top at the midsemispan station.

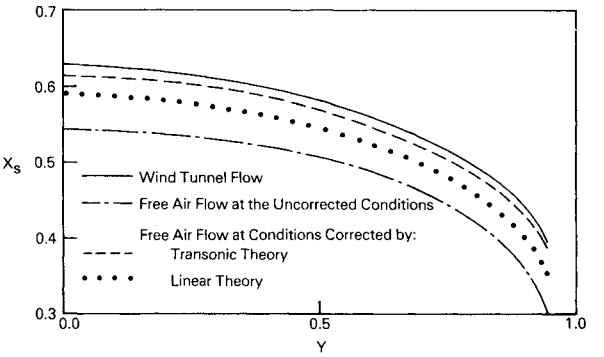

Fig. 6 Shock position on wing top.

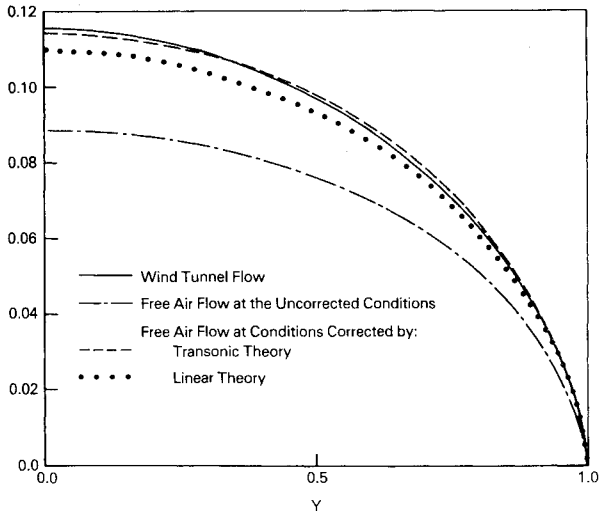

Fig. 4 Spanwise lift distribution.

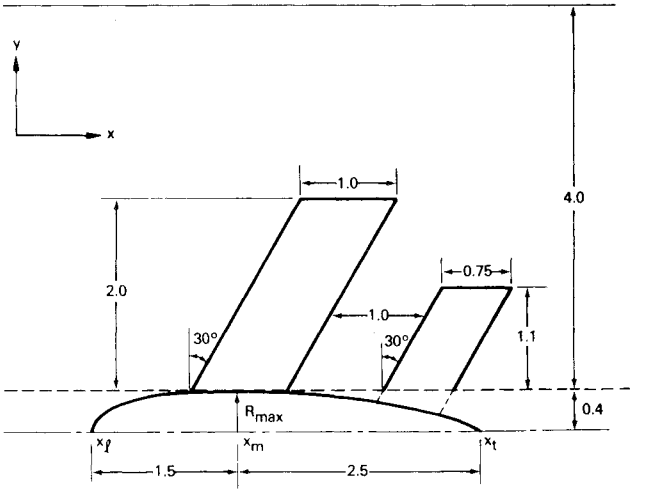

Fig. 7 Top view of model in tunnel.

For a wing model, the correction procedure applied here determines the Mach number and angle-of-attack corrections such that the model lift in free air and in the tunnel is matched, while the Mach number difference on the model surface in free air and in the tunnel is minimized. Alternative formulations determine the Mach number and angle-of-attack corrections such that the pressure difference[14] or the Mach number difference[25] on the model surface in the tunnel and free air is minimized with no constraints. In each of the formulations, the error function being minimized will not be equal to zero, in general, indicating that $\Delta\alpha$ and ΔM are only the lowest-order wall interference corrections. Higher-order corrections include lift, pitching moment, and drag corrections. If the data are correctable (i.e., the minimized error function is small), $\Delta\alpha$ and ΔM calculated by the present approach should agree to the lowest order with those calculated by the alternative approaches.[14,25] However, the main advantage of the present approach over the other approaches is its superior computational efficiency.

The correction procedure described above is applied to a wing-body-tail model configuration. The geometrical configuration of the model in a solid-wall wind tunnel is shown in Fig. 7. The model is assumed to be located at middistance between the tunnel upper and lower walls. The distance between these walls is 3.2 c. A NACA 0012 airfoil section is used for both the wing and tail. The body is axisymmetric and defined by

$$r = r^b = R_{\max}\sqrt{1-\left(\frac{x_m - x}{x_m - x_\ell}\right)^2} \qquad x_\ell \le x \le x_m$$

$$= R_{\max}\left[1-\left(\frac{x - x_m}{x_t - x_m}\right)^2\right] \qquad x_m \le x \le x_t$$

where r is the radial coordinate, and the coordinates x_ℓ, x_m, and x_t are defined in Fig. 7. The maximum body radius is taken to be 0.4. The undisturbed wind tunnel Mach number is assumed to be 0.77, while $L_{e,d}$ and $m_{e,d}$ are assumed to be 0.4 and 1.6, respectively.

A Cartesian computational mesh is used in the calculations. The small disturbance boundary conditions for the wing and tail are applied on planar mean surfaces in the usual manner. The body boundary conditions are also applied on the planar surfaces $y = W$ and $z = z_0 \pm H$ (see Fig. 8). For a general body the boundary condition at these surfaces is given by

$$\phi_N(x,\theta) = \phi_n(x,\theta)\,[s_\theta^b(\theta,x)/s_\theta^p(\theta)]$$

where $S^b(\theta,x)$ is the path length along the body cross-sectional contour at a given x station; $S^p(\theta)$ is the corresponding path length along the parallelepiped cross-sectional contour; n is the coordinate in the direction normal to the body contour; and N is the coordinate normal to the parallelepiped contour. In the special case of the axisymmetric body,

$$S_\theta^b = r^b \qquad n = r$$

The first step of the correction procedure determines the values of the wind tunnel angles of attack ($\alpha_{T,w} = 3.296$ deg, $\alpha_{T,t} = 3.780$ deg), while the second step determines the values of the corrected Mach number ($M_{F\infty} = 0.799$) and the corrected angles of attack ($\alpha_{F,w} = 4.212$ deg, $\alpha_{F,t} = 4.944$ deg). The values of $|E_M|$, $|E_{\alpha,w}|$, and $|E_{\alpha,t}|$ are reduced from

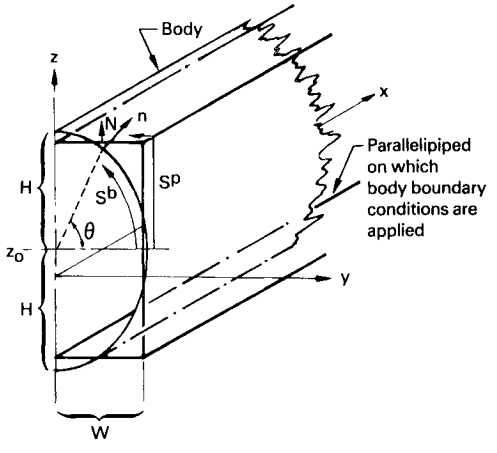

Fig. 8 Body and parallelepiped cross-sectional contours.

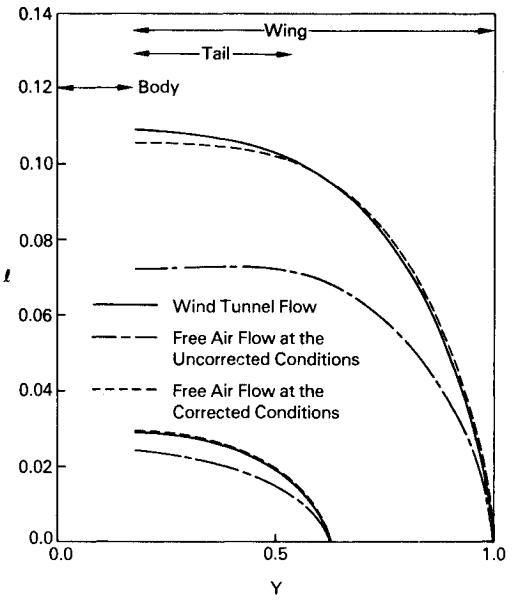

Fig. 9 Spanwise lift distribution for wing and tail.

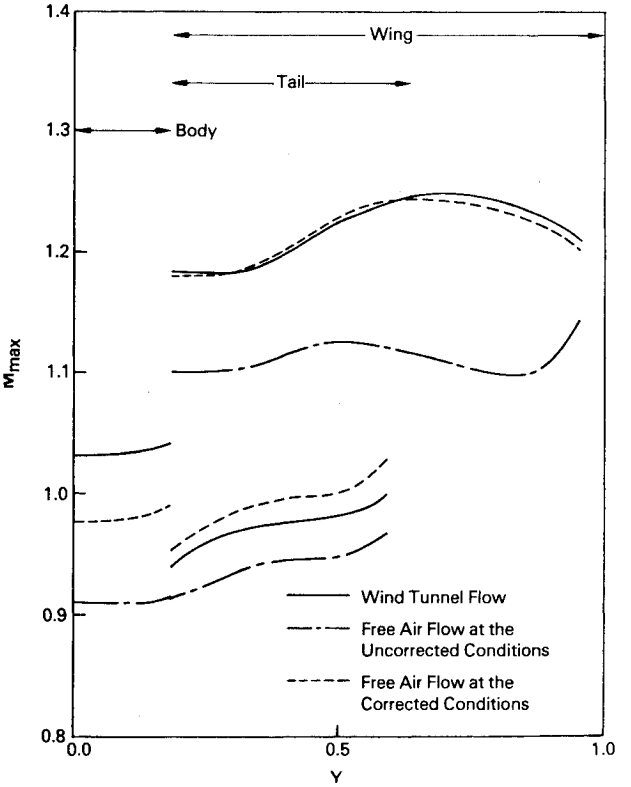

Fig. 10 Maximum Mach number distribution along wing top and tail top.

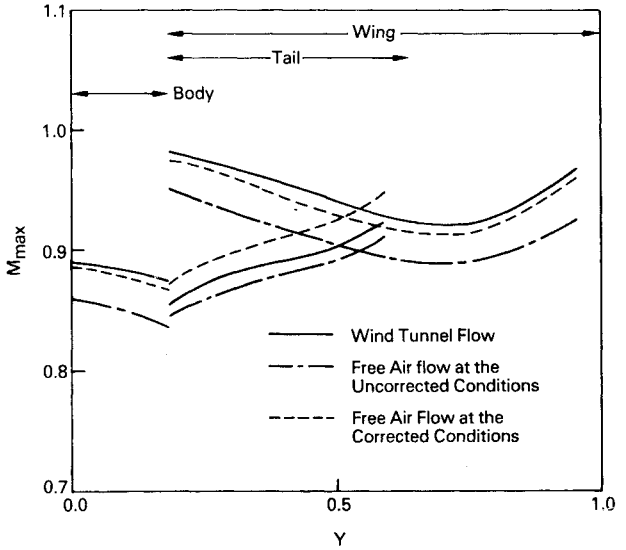

Fig. 11 Maximum Mach number distribution along wing bottom and tail bottom.

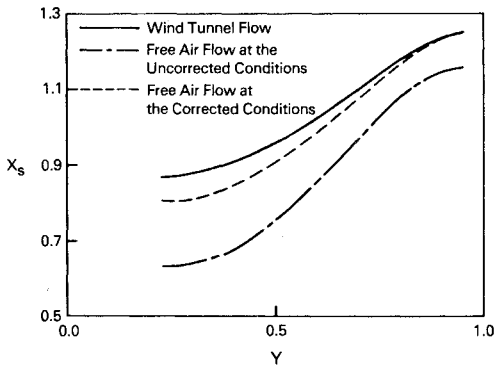

Fig. 12 Shock position on wing top.

0.393×10^{-2}, 0.296, and 0.211, respectively, for the flow at the uncorrected conditions to 0.519×10^{-3}, 0.276×10^{-4}, and 0.135×10^{-4}, respectively, for the flow at the corrected conditions.

A comparison between the spanwise lift distribution for the wind tunnel flow ($M_\infty=0.770$, $\alpha_w=3.296$ deg, $\alpha_t=3.780$ deg), the free-air flow at the corrected conditions ($M_\infty=0.799$, $\alpha_w=4.212$ deg, $\alpha_t=4.944$ deg), and the free-air flow at the uncorrected conditions ($M_\infty=0.770$, $\alpha_w=3.296$ deg, $\alpha_t=3.780$ deg) is given in Fig. 9. Figures 10 and 11 show the distribution of $M_{\max}$ (the maximum Mach number along a chord) along the wing and tail semispans on the top and bottom surfaces. These figures indicate that the blockage effect caused by the presence of the tunnel walls affects the different model components (wing, tail, and body) to different degrees of severity. It is therefore not possible to correct this effect uniformly on the different model components by a single blockage correction (ΔM). However, accurate blockage corrections for a specific component may be obtained by replacing the integrals in Eq. (3), which are taken over the model surface, by integrals taken over that component surface. A comparison between the shock wave locations for the different flow conditions is shown in Fig. 12.

In the above calculations, the initial guess for the values of $M_{F\infty}$, $\alpha_{F,w}$, and $\alpha_{F,t}$ were set equal to $M_{e\infty}$, $\alpha_{T,w}$, and $\alpha_{T,t}$, respectively. The initial incremental value $\delta M^1_{F\infty}$ and the constants c_1, c_2, and C_α were set equal to 0.002, 1.2, 0.6, and 3.0, respectively. The number of iterations required for convergence ($\epsilon_R=0.002$, $\epsilon_M=0.5\times10^{-5}$, $\epsilon_\alpha=0.5\times10^{-4}$) of the present iterative process is 104 iterations for the coarse mesh and 133 iterations for the fine mesh. The corresponding number of iterations required for convergence ($\epsilon_R=0.002$) of the standard iterative process ($\delta M^1_{F\infty}=C_\alpha=0$), with $M_{F\infty}=0.799$, $\alpha_{F,w}=4.212$ deg, $\alpha_{F,t}=4.944$ deg, is 110 iterations for the coarse mesh and 189 iterations for the fine mesh, indicating superior convergence properties for the present iterative process.

Conclusions

A method has been developed for the evaluation of wall interference corrections for three-dimensional aircraft configurations in the transonic regime. The corrected Mach number and angles of attack are those optimum values that minimize the Mach number difference on the model surface in the tunnel and free air while matching the lift and pitching moment. In addition to lift and pitching moment measurements, the procedure requires pressure measurements near the tunnel walls. An estimate of the accuracy of the correction is provided by the method.

The correction procedure, which has been formulated as an optimization problem, requires computation of the inviscid flow about the model in the tunnel and in free air. An efficient scheme that determines the solution of the flow equation and the corrected (optimum) values of the Mach number and angles of attack simultaneously has been developed.

Even though the present approach to the wall interference problem has been applied to geometrically simple test cases, and the governing equation is assumed to be the transonic small disturbance equation, the same approach may be used to solve problems of a geometrically complex nature and problems which require the use of the full potential equation or more complex equations.

The numerical examples presented here indicate that the correction procedure predicts Mach number and angle-of-attack corrections with good accuracy. Further calculations and the use of real experimental data are required to evaluate the present approach further.

Appendix: Evaluation of Wing and Tail Lifting Forces

The iterative procedure used in determining $\alpha_{T,w}$ and $\alpha_{T,t}$ requires that estimates be made for $L_{e,w}$ and $L_{e,t}$. The values of $L_{e,w}$ and $L_{e,t}$ satisfy the set of equations

$$L_{e,w}+L_{e,t}=L_{e,d} \tag{A1}$$

$$\xi_w L_{e,w}+\xi_t L_{e,t}=m_{e,d} \tag{A2}$$

where

$$\xi_w=x_m-x_w \qquad \xi_t=x_m-x_t$$

and x_w and x_t are the x coordinates of the center of forces on the wing and tail, respectively. Since ξ_w and ξ_t are not given, they are estimated at each iterative step. An the nth iterative step, they are given by

$$\xi^n_w=m^n_{T,w}/L^n_{T,w} \qquad \xi^n_t=m^n_{T,t}/L^n_{T,t}$$

These estimates are substituted into Eqs. (A1) and (A2) to obtain the following values for $L_{e,w}$ and $L_{e,t}$ at the nth iteration

$$L^n_{e,w}=\frac{\xi^n_t L_{e,d}-m_{e,d}}{\xi^n_t-\xi^n_w} \qquad L^n_{e,t}=\frac{m_{e,d}-\xi^n_w L_{e,d}}{\xi^n_t-\xi^n_w}$$

Acknowledgment

This work was supported by NASA Langley Research Center under Contract NAS1-16262.

References

[1]Garner, H.C., Rogers, E.W.E., Acum, W.E.A. and Maskell, E.C., "Subsonic Wind Tunnel Wall Corrections," AGARDOgraph 109, Oct. 1966.

[2]Sears, W.R., "Self Correcting Wind Tunnels," *The Aero Journal,* Vol. 78, Feb./March, 1974, pp. 80-89.

[3]Ferri, A. and Baronti, T., "A Method for Transonic Wind Tunnel Corrections," *AIAA Journal,* Vol. 11, Jan. 1973, pp. 63-66.

[4]Kraft, E.M. and Parker, R.L., "Experiments for the Reduction of Wall Interference by Adaptive-Wall Technology," AEDC-TR-79-51, Oct. 1979.

[5]Parker, R.L. and Sickles, W., "Application of Adaptive Wall Techniques in a Three Dimensional Wind Tunnel with Variable Porosity," AIAA Paper 80-157, Jan. 1980.

[6]Erickson, J.C., Wittliff, C.E., Padova, C. and Homicz, G.F., "Adaptive Wall Wind Tunnel Investigations," CALSPAN Report RK-6040-A-2, Feb. 1981.

[7]Bernstein, S. and Joppa, R.G., "Development of Minimum Correction Wind Tunnels," AIAA Paper 75-144, Jan. 1975.

[8]Bodapati, J., Schairer, E., and Davis, S., "Adaptive Wall Wind Tunnel Development for Transonic Testing," AIAA Paper 80-0441, March 1980.

[9]Goodyear, M.J. and Wolf, S.W.D., "The Development of a Self-Stream-lining Flexible Walled Transonic Test Section," AIAA Paper 80-0440, March 1980.

[10]Chevallier, J.P., "Souflerie transsonique a porois auto-adaptables," AGARD CP-174-12, Oct. 1976.

[11]Ganzer, U., "Adaptable Wind Tunnel Walls for 2D and 3D Model Tests," ICAS Conference Proceedings Paper 23.3, Munich, F.R.G., 1980.

[12]Kemp, W.B. Jr., "Toward the Correctable-Interference Transonic Wind Tunnel," AIAA 9th Aero Testing Conference, June 1976, pp. 31-38.

[13]Kemp, W.B. Jr., "Transonic Assessment of Two-Dimensional Wind Tunnel Wall Interference Using Measured Wall Pressures," NASA CP-2045, March 1978, pp. 473-486.

[14]Murman, E.M., "A Correction Method for Transonic Wind Tunnel Wall Interference," AIAA Paper 79-1533, July 1979.

[15]Rizk, M.H. and Smithmeyer, M.G., "Wind-Tunnel Wall Interference Corrections for Three-Dimensional Flows," *Journal of Aircraft,* Vol. 19, June 1982, pp. 465-472.

[16]Rizk, M.H., "Higher-Order Flow Angle Corrections for Three-Dimensional Wind Tunnel Wall Interference," *Journal of Aircraft,* Vol. 19, Oct. 1982, pp. 893-895.

[17]Mokry, M., "Subsonic Wall Interference Corrections for Finite Length Test Sections using Boundary Pressure Measurements," Paper 10, AGARD Fluid Dynamics Panel Specialists' Meeting on Wall Interference in Wind Tunnels, May 1982.

[18]Mokry, M. and Ohman, L.H., "Application of the Fast Fourier Transform to Two-Dimensional Wind Tunnel Wall Interference," *Journal of Aircraft,* Vol. 17, June 1980, pp. 402-408.

[19]Davis, S.S., "A Compatibility Assessment Method for Adaptive-Wall Wind Tunnels," *AIAA Journal,* Vol. 19, Sept. 1981, pp. 1169-1173.

[20]Rizk, M.H., Hefez, M., Murman, E.M., and Lovell, D., "Transonic Wind Tunnel Wall Interference Corrections for Three-Dimensional Models," AIAA Paper 82-0588, March 1982.

[21]Rizk, M.H., "Propeller Slipstream/Wing Interaction in the Transonic Regime," *Journal of Aircraft,* Vol. 18, March 1981, pp. 184-191.

[22]Isaacson, E. and Keller, H.B., *Analysis of Numerical Methods,* John Wiley & Sons, New York, 1966, pp. 96-97.

[23]Rizk, M.H., "A New Approach to Optimization for Aerodynamic Applications," *Journal of Aircraft,* Vol. 20, Jan. 1983, pp. 94-96.

[24]Rizk, M.H., "A New Optimization Technique Applied to Wind Tunnel Angle-of-Attack Corrections," Flow Industries, Inc., Kent, Wash., Research and Technology Division, Note 198, Feb. 1982.

[25]Rizk, M.H., "The Single-Cycle Scheme—A New Approach to Numerical Optimization," Flow Industries, Inc., Kent, Wash., Research and Technology Division, Report 243, Sept. 1982.